

**●Original Contribution****ULTRASOUND TISSUE DISPLACEMENT IMAGING WITH
APPLICATION TO BREAST CANCER**

E. J. CHEN,[†] R. S. ADLER,[‡] P. L. CARSON,[‡] W. K. JENKINS[†]
and W. D. O'BRIEN, JR.[†]

[†]Department of Electrical and Computer Engineering, University of Illinois at Urbana-Champaign, Urbana, IL, USA and [‡]Department of Radiology, University of Michigan Hospitals, Ann Arbor, MI, USA

(Received 4 July 1994; in final form 5 May 1995)

Abstract—A method for quantitative imaging of internal tissue motion based on speckle tracking is described. Tissue displacement images from eight patients with sonographically apparent breast masses are used to illustrate the technique. The local displacement response of tissues surrounding malignant and benign breast masses is compared, testing the hypothesis that altered mechanical properties may result in motion signatures for many soft tissue tumors relative to their host tissue. In addition, the potential or anticipated influence of various biological and physical factors on tissue motion response is discussed.

Key Words: Tissue motion, Stellate, Tissue displacement, Displacement imaging.

INTRODUCTION*Motivation*

Recent studies indicate that breast cancer affects one of every eight women in the United States (American Cancer Society 1991). Early detection can greatly improve a woman's chances for survival (Kimme-Smith 1992). It is estimated that approximately 20% of breast cancers are missed in conventional mammographic screening (Martin et al. 1979). Several risk factors for breast cancer have been identified (Berg 1984). These include family history, nutrition and exposure to radiation. Yet, in almost 75% of women with breast cancer, none of these factors is present (Berg 1984). While not present in all mammograms, the presence of a stellate mass in the breast is one of the most distinct mammographic characteristics of a breast malignancy (Ciatto et al. 1993; Krecke and Gisvold 1993; Leibman et al. 1993; Martin et al. 1979; McLelland 1990; Monostori et al. 1991; Sickles 1984).

Physiology of malignant breast masses

It is believed that cancer cells in the breast stimulate the growth of fibrous tissues. This pattern of

growth, termed desmoplastic reaction, is what gives malignant breast masses a dense or hard consistency. Carcinoma cells grow in the path of least resistance. When the surrounding tissues are firm and have a mostly glandular constituency, as found in younger women, the tumor cells tend to grow in clefts between fibrous regions. When the surrounding tissues are soft and have a more fatty consistency, tumor cells grow in all directions. Many primary malignancies exhibit a stellate (star-shaped) pattern or spiculated appearance (Ciatto et al. 1993; Krecke and Gisvold 1993; Monostori et al. 1991). The spiculated appearance of many malignant masses in the breast, with tentacles radiating outward from the tumor into surrounding tissues, is well documented in the literature (Bogaert and Herman 1977; Gallagher and Martin 1969; Gold and Bassett 1981; Heitzman 1973; Leborgne 1951; Leibman et al. 1993; Moskowitz 1979; Tabar and Dean 1985; Wolfe 1983).

Drawings of idealized infiltrative and benign primary breast lesions are shown in Fig. 1 (adapted from Ueno 1986). The infiltrative malignant mass is characterized by a stellate configuration with spicules and is reasonably typical of invasive ductal carcinoma. In other cases, the invasion may have longer stellate radial arms due to desmoplastic reaction between the surrounding tissue and the tumor and may include invasion along ducts and other connective tissue surfaces.

Address correspondence to: Professor William D. O'Brien, Jr., Department of Electrical and Computer Engineering, University of Illinois, 1406 West Green Street, Urbana, IL 61801, USA. e-mail: wdo@uiuc.edu.

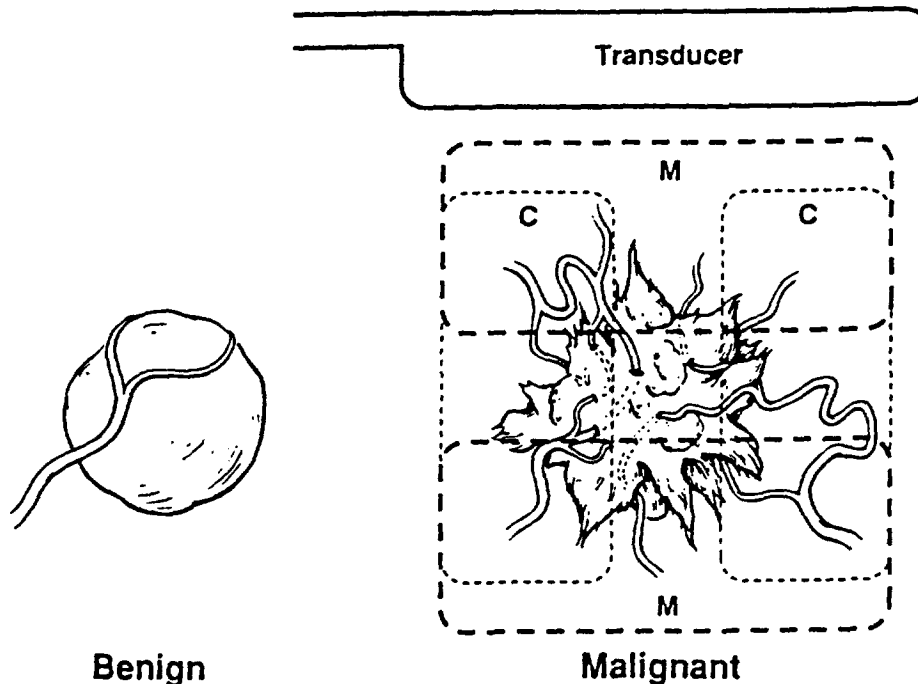


Fig. 1. Drawings of idealized malignant and benign breast masses.

The degree of desmoplastic reaction or deformation of surrounding tissues due to bonding between the tumor and connective tissues will alter the tumor and connective tissue responses to palpation. Ultrasound provides a method for real-time imaging of local tissue motion, which may be helpful in diagnosing breast cancer (Ueno et al. 1988). Ultrasonic measurement of local tissue motion provides a means of quantifying tumor and connective tissue responses to palpation. This information could be potentially used in the early detection and classification of many developing breast cancers.

Desmoplastic reaction may also alter the mechanical and thus tissue-elastic properties of invaded areas. Ultrasonic elasticity imaging, which involves noninvasive ultrasonic measurement of tissue elastic properties, has also been demonstrated as a viable means of imaging small, totally nonpalpable objects in simulated gel phantoms of the breast (Cespedes et al. 1993; O'Donnell et al. 1994; Ophir et al. 1991; Skovoroda et al. 1994).

Feasibility of ultrasonic speckle tracking to measure internal tissue displacements

A two-dimensional ultrasonic speckle tracking system capable of displaying tissue motion in the form of 1D and 2D displacement and velocity vectors and color maps of these vectors has been developed in the

Bioacoustics Research Laboratory at the University of Illinois. The system was used to measure palpated tissue motion in eight patients with both benign ($n = 5$) and malignant ($n = 3$) breast masses, testing the hypothesis that altered mechanical properties may result in motion signatures for many tumors relative to their host tissue.

A 2D correlation-based speckle tracking algorithm was used to ultrasonically track tissue displacements (Hein and O'Brien 1993). The tissue speckle tracking procedure has been demonstrated to be feasible to both accurately and precisely measure local tissue motion (Hein and O'Brien 1993; Ramamurthy and Trahey 1991), thus providing a way to compare normal and malignant breast tissue motion both quantitatively and qualitatively.

Internal tissue displacements were computed from sequential acquired ultrasound images using the following four-step tissue speckle tracking procedure.

1. A tissue region of interest (ROI) is selected from the initial ultrasound scan.
2. The ROI is compared with identically sized templates inside of a predefined search region in a successive ultrasound scan.
3. At each position in the search region, a normalized correlation coefficient [eqn (1)] is computed between the ROI and the template.

$$\rho_{xy}(k, l) = \frac{\sum_{i=1}^M \sum_{j=1}^N (x(i, j) - \bar{x}) \times (y(i + k, j + l) - \bar{y})}{\sqrt{\sum_{i=1}^M \sum_{j=1}^N (x(i, j) - \bar{x})^2} \sqrt{\sum_{i=1}^M \sum_{j=1}^N (y(i + k, j + l) - \bar{y})^2}} \quad (1)$$

4. The template producing the largest correlation coefficient is assumed to be the new location of the ROI. A two-dimensional displacement vector is computed for the ROI.

In eqn (1), $x(i, j)$, $y(i, j)$ represent the pixel intensities in the ROI and template, M and N represent the horizontal and vertical dimensions of the ROI and template, the variables (k, l) represent the pixel coordinates of the template region in the second image and \bar{x} , \bar{y} are the mean pixel values in the ROI and template. Displacement vectors are assumed to start in the center of ROIs and all pixels in the ROI are assumed to translate by the magnitude and direction of the displacement vector. The procedure can be repeated to incrementally track local tissue displacements through a sequence of ultrasound images. A full description of the 2D correlation-based tissue tracking technique is also provided in several earlier references (Chen *et al.* 1991; Hein and O'Brien 1993).

Accuracy of ultrasonic tissue tracking

The accuracy of ultrasonic tissue tracking has been investigated in depth (Chen *et al.* 1994; Ramamurthy and Trahey 1991). Previous studies using a computer-controlled positioning system have indicated that regions as small as 1.0 mm can be tracked with less than 5% error for displacement distances exceeding 20.0 mm under appropriate conditions. Tissue tracking performance has been observed to be better in heterogeneous tissues such as muscle, which contain well-defined fibers and other internal tissue structure; tracking performance deteriorated in homogeneous tissues such as liver (Chen *et al.* 1992).

The effect of six different imaging parameters on ultrasonic displacement tracking has also been studied (Chen *et al.* 1994). The demonstrated accuracy with which ultrasonic tissue speckle tracking can be used to measure local tissue displacements thus provides a technique by which malignant and benign breast tissue motion can be analyzed both quantitatively and qualitatively. It should be stressed that the focus of this study is the tissue displacement imaging technique, with the

motion responses of breast tumors used only as an example of a potentially useful application.

METHODS

High-frequency ultrasound images of malignant and benign breast masses were acquired from eight patients seen in the Department of Radiology at the University of Michigan Hospital. Information regarding patient age, menopausal status, type and size of mass and biopsy type and results are shown in Table 1. Patients were scanned using a 7.5-MHz linear array transducer (Acoustic Imaging, Phoenix, AZ). The transducer was used to perform palpation with the patient supine and the breast stationary. In each case, the patient's arm was placed above the head on the side scanned. In this article, the term "palpation" is used to denote a translational motion of the imaging transducer over the breast accompanied by a hand-rocking motion by the physician. The transducer was translated opposite to the direction of palpation, imparting a small shearing force on the parenchymal tissue directly above mass. We were particularly interested in tracking the motion of parenchymal tissue adjacent to and above masses to see if this could provide a motion signature for each mass. We specifically examined the interface between masses and adjacent tissue in terms of a motion gradient as a possible means to separate infiltrative and noninfiltrative abnormalities. All examinations were performed with informed consent of patient volunteers, under protocols approved by the institutional review board. Breast masses were diagnosed based on ultrasound, mammography and biopsy results.

Sonographic features considered in diagnosing benign masses included homogeneity of internal echoes, good margination or definition of edges, nonattenuation of sound through-transmission of the mass and the presence of strong anterior echoes, whereas features used in diagnosing malignancy included irregular margination of masses, laterally dense boundary echoes (halo), rough or jagged borders and the presence of posterior shadowing (Bamber *et al.* 1988; Kasumi *et al.* 1982; Ueno 1993; Ueno *et al.* 1988; Vlajavljovic 1988). The composition of the breast parenchymal tissues was also characterized for each patient, based on mammography and ultrasound data, unless otherwise stated.

Continuous ultrasonic scans of the resulting breast tissue motion were recorded on standard VHS videotape. Serial frames of breast tissue motion through a single palpation cycle were digitized using a commercially available Targa version 2.0 framegrabbing sys-

Table 1. Patient information.

Patient #	Age	Menopausal status	Mass type	Biopsy type	Mass diameter
1	42	Pre-	Fibrocystic	Excisional	3.0 mm
2	46	Pre-	Fibrocystic	Aspiration	10.0 mm
3	30	Pre-	Fibroadenoma	Aspiration	40.0 mm 20.0 mm
4	59	Post-	Fibrocystic	Aspiration	13.0 mm
5	35	Pre-	Breast nodule	None	7.0 mm
6	43	Pre-	Amelanotic melanoma	Excisional	4.8 mm
7	64	Post-	Invasive ductal carcinoma	Excisional	18.0 mm
8	78	Post-	Invasive ductal carcinoma	Excisional	3.7 mm

tem (Truevision). The digitized gray scale images were ported to a Sun Sparc2 workstation for analysis.

To generate a color map of tissue displacement, a rectangular grid of equally spaced points was centered on the lesion in the first frame of the image sequence. A rectangular kernel region was centered on each grid point and the displacement of each kernel region was tracked through the image sequence. By tracking the displacement of various kernels or regions of tissue at each grid point in the field, a map of displacement vectors representing the tissue displacement field can be generated. The effect of different kernel sizes and grid spacings is discussed later. Qualitative color maps were used to display tissue displacement fields. Quantitative information was obtained by plotting a cross-sectional slice of the color map. To simplify the display of tissue displacement fields only the lateral component of tissue motion, which was the same as the direction of palpation, is shown. Blue areas indicate small tissue displacements (0.0 to 10.0 mm), yellow areas indicate moderate tissue displacements (10.0 to 17.0 mm) and red areas indicate large tissue displacements (17.0 to 25.0 mm). The system allows the user to specify the desired spacing between grid points, kernel dimensions and number of frames in the image sequence. The system requires approximately 45 s to compute the displacement of a single ROI with dimensions of 3.75 cm \times 1.25 cm through a sequence of three images.

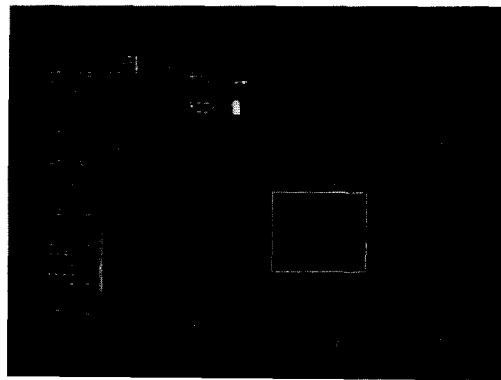
RESULTS

Gray scale findings

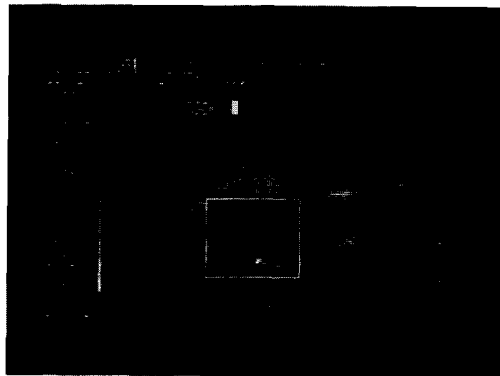
The results of this section include findings from ultrasound and mammography data. Figure 2a shows an ultrasound scan of normal breast tissue containing a benign cyst (patient 1, Table 1). The mass is well marginated and anechoic with a well-defined posterior margin and enhanced through-transmission, all classic sonographic features of a benign cyst. Figure 2b is a scan of the same plane of the breast at the end of palpation by the physician. The position of the cyst

pinpointed by the correlation search algorithm is highlighted. Motion of a cyst can be seen in ultrasound B-scan images if the cyst is palpated by standard hand techniques. Figure 2c indicates the initial and final position of the cyst shown in Fig. 2a and of a section of tissue adjacent to the mass. From Fig. 2c, it is apparent that there is significant displacement of the lesion due to palpation, but only minimal displacement of the adjacent parenchymal tissue proximal to the transducer.

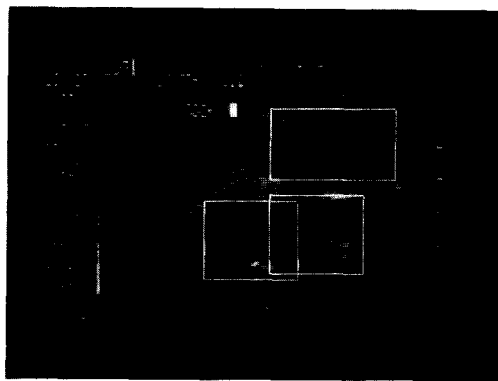
Gray scale ultrasound scans for eight patients with breast masses are shown in Fig. 3. Patient information and biopsy results are summarized in Table 1 and Fig. 3a-h are from patients 1 to 8, respectively. Patients 1 to 5 all had solid benign masses based on imaging and biopsy results. Benign imaging features, as discussed earlier, included homogeneity of internal echoes, good margination of edges and nonattenuation of sound through the nodule. The presence of strong posterior echo levels in patients 1 and 2 and strong anterior echo levels in patient 3 are also typical of benign breast disease, although an area of posterior shadowing was observed below the right mass in patient 3. Mammography results for patient 3 indicated the presence of three nodular densities in the left breast with no suspicious calcifications. A limited ultrasound of the upper, outer quadrant of the left breast in the region of the nodular opacities (Fig. 3c) revealed two of the solid masses corresponding to the nodules on the mammogram. The largest nodule is indicated by the arrow in Fig. 3c. Needle aspiration biopsy results for patients 1 and 2 indicated that they were benign fibrocystic masses, whereas needle aspirational biopsy results for patient 3 revealed myoepithelial cells consistent with fibroadenoma. A single 4.2 cm \times 3.2 cm \times 1.4 cm tissue specimen from patient 1 was also submitted for histological examination. Sectioning revealed a composition of roughly 80% adipose, with one end of the specimen diffusely fibrous and containing a 3.0-mm fluid-filled cyst region. The character of the surrounding parenchymal tissue in patient 3 was noted to



a)



b)



c)

Fig. 2. (a) Diagnostic ultrasound image of a benign complex cyst from patient 1 (determined from needle aspiration) at the start of palpation. This mass has well defined posterior wall with signal enhanced through-transmission. (b) Diagnostic ultrasound image of the same complex cyst at the end of palpation. The position of the cyst as tracked by the correlation search algorithm is highlighted by the rectangular box. (c) Position of the fibrocystic mass and adjacent tissue before and after palpation.

be composed of a mixture of fatty and fibroglandular tissue based on mammography data and ultrasound images.

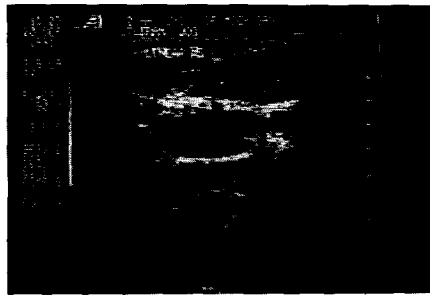
Needle aspiration biopsy results for patient 4 indicated a benign fibrocystic mass. Patient 5 had irregular margination with the suggestion of posterior shadowing. No biopsy was performed on patient 5; however, this patient was mammographically stable for more than 4 years. The breast parenchyma in patient 4 was characterized as being composed of nodular, moderately dense fibroglandular tissue, whereas the parenchymal tissue in patient 5 was noted to be composed of predominantly fatty tissues with a small amount of residual fibroglandular tissue.

The lesion in patient 6 appeared to have inhomogeneities of internal echoes with some suggestion of areas of necrosis. Excisional biopsy results for patient 6 indicated it was a metastatic amelanotic melanoma. The lesions in patients 7 and 8 were irregular margined masses that appeared to drag adjacent parenchyma when palpated. They had posterior shadowing, halo and other classic sonographic features of malignancy described earlier. Excisional biopsy results for patients 7 and 8 indicated that they were both invasive ductal carcinomas. The breast parenchyma for patient 6 was characterized as being composed of predominantly fatty tissues, whereas patients 7 and 8 were reported to be composed of mixed fatty and fibroglandular tissues.

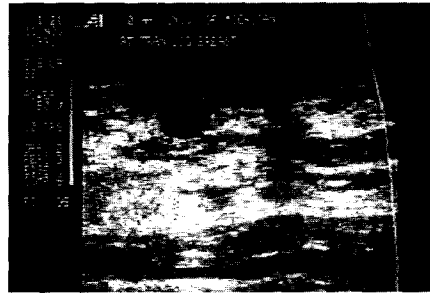
Displacement maps

Ultrasound computed displacement maps, shown in Fig. 4, were generated using a field grid spacing of 0.25 mm per pixel. In each case, a rectangular kernel with dimensions approximately equal to the size of the lesion area was used in the correlation tracking. The grid spacing, field sizes and kernel sizes used for all patients are summarized in Table 2.

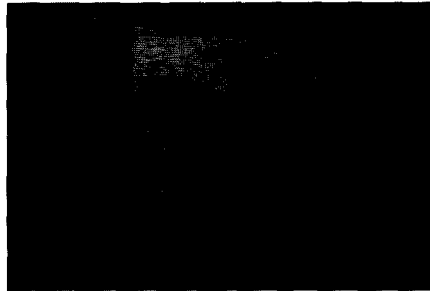
Figure 4a–g shows color maps of the tissue displacement field for the corresponding masses seen in Fig. 3a–g for patients 1 to 8, respectively. Each displacement field consists of a 100 × 100 grid of points or displacement vectors centered on the lesion at the start of palpation. A 50 × 100 grid was used for patients 4 and 7 because of the smaller available field of view in the ultrasound images. The orientation of the color maps is the same as that used in the diagnostic ultrasound scans with top to bottom corresponding to depth or axial distance from the transducer and left to right corresponding to the direction lateral to the beam axis. All palpations were from the left to right direction. Based on the palpation applied (translational motion of the transducer over breast masses), three types of motions were observed and these included: (1) slip



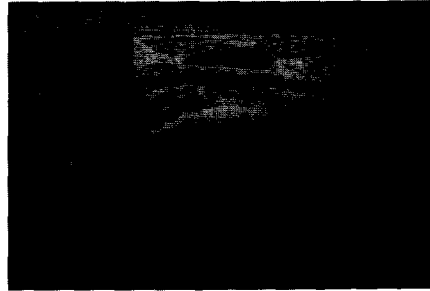
a) patient 1



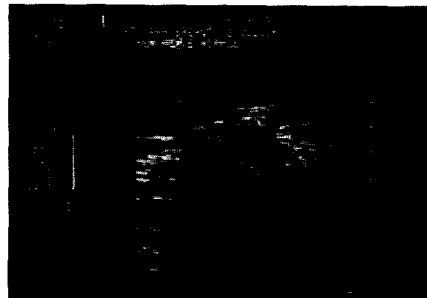
b) patient 2



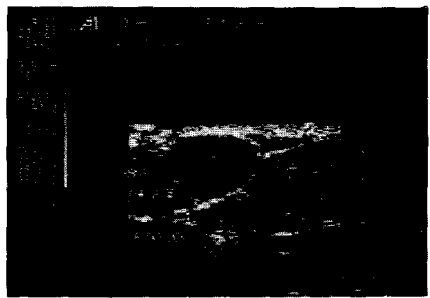
c) patient 3



d) patient 4



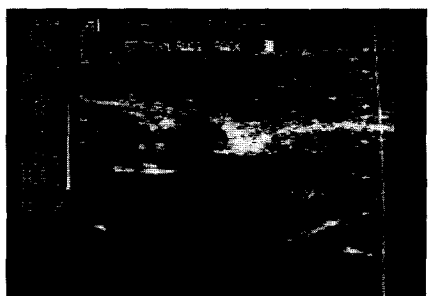
e) patient 5



f) patient 6



g) patient 7



h) patient 8

Fig. 3. Diagnostic ultrasound scans of eight patients with varying degrees of breast disease. (a) Elliptically shaped benign complex cyst (determined from excisional biopsy). (b) Circularly shaped benign complex cyst (determined from needle aspiration). (c) Benign fibroadenoma (determined from needle aspiration) with nodule indicated by arrow. (d) Elliptically shaped fibrocystic mass (determined from needle aspiration). This cyst is near the chest wall, reducing significant enhancement through-transmission. (e) Benign fibroadenoma (diagnosis based on imaging). Mass is indicated by arrow. *Note:* Patient was mammographically stable for greater than 4 years. (f) Amelanotic melanoma (based on excisional biopsy). (g) Infiltrating ductal carcinoma (based on excisional biopsy). Mass indicated by arrow. Both carcinomas, (g) and (h), are poorly defined shadowing lesions, that appeared to drag adjacent parenchyma when palpated. They had posterior shadowing, halo and irregular margination, all classic indicators of malignancy. (h) Infiltrating ductal carcinoma (based on excisional biopsy).

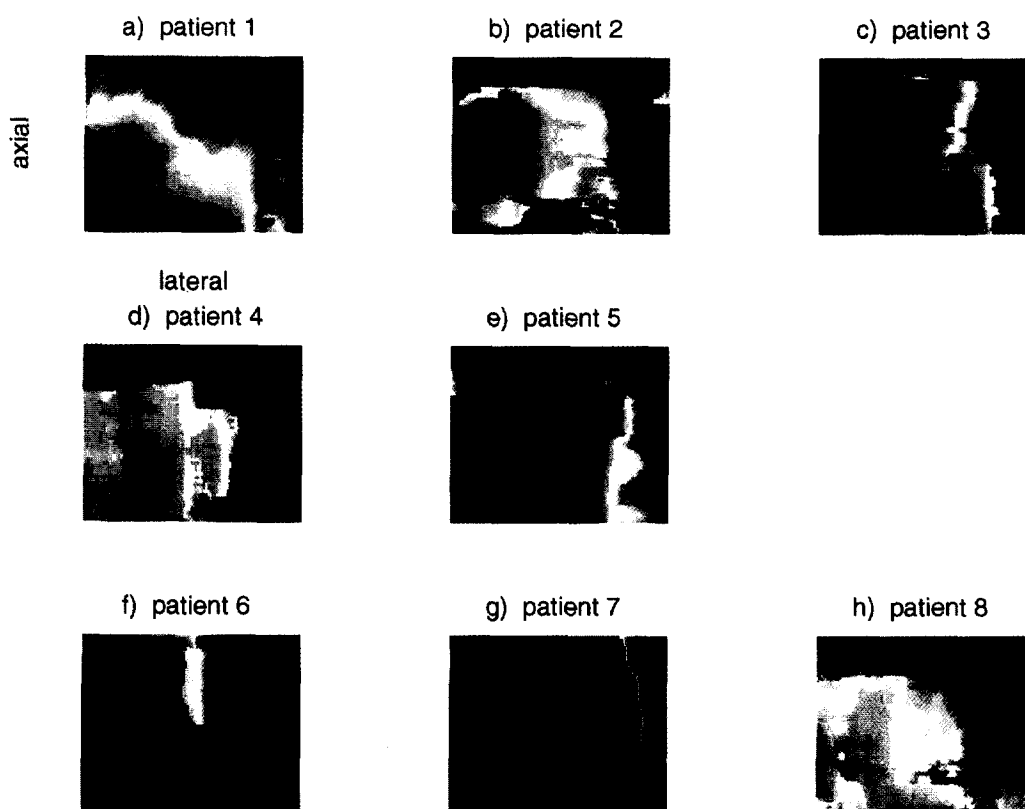


Fig. 4. (a–e) Tissue displacement fields for benign fibrocystic masses and fibroadenomas of patients 1 through 5, respectively. Blue, yellow and red areas correspond to small (0.0 to 10.0 mm), medium (10.0 to 17.0 mm) and large (17.0 to 25.0 mm) displacements. The presence of a blue–red border indicates discontinuous motion between mass and adjacent tissue. Such a feature would be typical of a slip boundary. A 50×100 point grid was used for the displacement field due to the position of the lesion near the top of the ultrasound scan in Fig. 3d. (f–h) Displacement fields for the metastatic amelanotic melanoma and infiltrating ductal carcinomas of patients 6 through 8. The large extent of the red regions in patients 6 and 7 indicates fixed translational motion of the mass and surrounding tissue.

motion (shear motion of adjacent tissue above mass, opposite to the direction of palpation); (2) slight drag (small displacement of adjacent tissue in the direction of palpation); and (3) fixed translation (*en bloc* displacement of mass and adjacent parenchyma).

Color maps of tissue displacement fields exhibited regions of red, then yellow, then blue when looking across the color map from left to right. This indicates that the largest tissue displacement occurred for tissues on the left side of tumors and that small displacements occurred in the tissues on the right side of tumors. This is consistent with the left-to-right palpation and the fact that tissues closest to the point of palpation contact should translate the most, whereas tissues farthest away should translate the least. In Fig. 4c, the presence of the blue band on the left side of the color map represents the left side of the image in Fig. 3c. Because the starting position of the mass in Fig. 3c was on the left edge of the image, displacement of tissues to the far left of the lesion could not be estimated.

To obtain a more quantitative measure of tissue motion, the average displacement for each patient was computed along the center axial slice of each displacement field. The average displacement was computed in two windows. Window A extended from a depth of 0 to 25 pixels (6.25 mm) and is representative of tissue motion directly above masses. Since the transducer was used to impart a shear force on the tissue directly above masses, motion in this region was of particular interest. Window B extended from a depth of 25 to 100 pixels (18.75 mm) and is representative of the displacement of masses. The adjacent tissue displacement (window A) and mass displacement (window B) for all patients are presented in Table 3.

DISCUSSION

The limited resolution of ultrasound does not allow imaging of any possibly invasive tentacles extending from a tumor site. However, imaging of tissue

motion can provide important clues in the early detection of invasive tumor growth into surrounding tissues. The cystic mass in Fig. 2 displayed discontinuous motion between the mass and adjacent tissue. Such a feature would be typical of a slip boundary and was present in all cases of fibrocystic disease.

It would be diagnostically useful for a physician to observe the motion of surrounding tissue as a lesion is palpated, because many breast cancers, such as schirous carcinoma, infiltrate into surrounding tissues. Palpation of these cancers results in apparent dragging of the adjacent parenchymal tissues. Ultrasound tracking of tissue motion provides a strong tool in aiding the physician in observing motion of adjacent parenchymal tissues, and in reducing errors due to visual errors and artifacts.

Three basic types of motion were observed (slip, slight drag, fixed translation) and consistent with the physiological growth patterns of masses and histological information discussed earlier. A red-blue border was visible in all five benign masses indicating discontinuous motion and consistent with a slip boundary. The presence of light blue regions in patients 5 and 8 (Fig. 4) indicates a slight drag with small displacement of adjacent tissue following palpation of the mass. Patients 6 and 7 (Fig. 4) depict fixed translational motion, with *en bloc* motion of adjacent parenchyma as the mass is palpated and suggestive of an infiltrative component to the mass. This was consistent with histology results which indicated invasive ductal carcinoma and was also compatible with margins seen on mammography.

In the present study, the transducer was used to impart a shear force on the tissue directly above masses. We were particularly interested in tracking tissue motion in this area to investigate the premise that infiltrating malignancies might alter motion responses. Based on our limited patient size, we observed an increased adjacent tissue displacement for malignant masses. This difference was particularly noticeable for patients 6 and 7 relative to the benign masses (Table 3). Although there is considerable variability between

Table 3. Mean adjacent tissue and mass displacement.

Patient #	Mass type	Adjacent tissue displacement (pixels)	Mass displacement (pixels)
1	Benign	28	43
2	Benign	13	46
3	Benign	34	57
4	Benign	25	41
5	Benign	10	54
6	Malignant	44	56
7	Malignant	53	60
8	Malignant	14	40

patients and masses, our results suggest that palpation of malignancies can result in dragging or fixed translation of adjacent parenchyma, consistent with qualitative expectations. Future studies with larger population sizes will be necessary to ultimately determine if there is a statistical trend toward more translation for malignancies. A normalized index such as relative adjacent tissue motion per mean mass displacement may also be useful, since this would roughly quantitate the percent drag of masses and adjacent parenchyma.

The quantitative characterizations of the motions observed are consistent with the qualitative results seen in previous studies (Adler et al. 1990; Leucht et al. 1988; Ueno 1986). The present motion analysis also better defines such motion and perhaps more importantly may eventually allow the remote characterization of lesion boundaries in deeply situated lesions, even with relatively small displacements, based on the ability of speckle tracking algorithms to track relatively fine motions (Hein and O'Brien 1993).

All five benign fibrocystic masses produced motions as might be expected for slip boundaries or no particular anchoring to surrounding tissues. Tissue displacement images exhibited fixed translational motion for two of the three malignant tumors.

For color maps of tissue displacement, selecting small kernel dimensions provides more localized motion information. However, the accuracy of correlation tracking is generally inversely proportional to the kernel size (Chen et al. 1994). Thus, resolution or localization of motion information is traded off against accuracy of results as kernel dimensions are adjusted. The grid spacing can be made arbitrarily small by simply increasing the total number of grid points (and reducing the distance between grid points). The grid spacing is ultimately limited only by the pixel resolution of the digitized ultrasound images (0.25 mm per pixel). A smaller grid spacing will provide a higher spatial resolution in maps of tissue displacement and velocity. However, the resulting increase in grid points will require additional computations.

Table 2. Displacement tracking parameters.

Patient #	Field size (points)	Grid spacing	Kernel dimensions
1	100 × 100	0.25 mm	25.0 mm × 12.5 mm
2	100 × 100	0.25 mm	10.0 mm × 10.0 mm
3	100 × 100	0.25 mm	25.0 mm × 12.5 mm
4	50 × 100	0.25 mm	18.7 mm × 6.3 mm
5	100 × 100	0.25 mm	15.0 mm × 12.5 mm
6	100 × 100	0.25 mm	20.0 mm × 15.0 mm
7	50 × 100	0.25 mm	12.5 mm × 15.0 mm
8	100 × 100	0.25 mm	10.0 mm × 8.8 mm

The preliminary results in this article are intended as a demonstration of the tissue displacement imaging technique. Displacement fields from breast tumors are used to demonstrate a potentially useful application of the method. It must be stressed that there are many biological and physical factors which can influence the connective tissue motion response to palpation. The structure of the parenchymal tissue surrounding the breast mass can alter the degree of motion response. In addition, the motion response from a stellate mass in a 40-year-old premenopausal patient can be expected to be different than the motion response of the same mass in a 75-year-old patient.

The position of the patient during examination and location of the mass within the breast is also important and can influence the motion response to palpation. For example, a thin mass located in a lateral plane or in the lateral aspect of the breast may require a patient to be rotated on her hip to obtain a reasonable image of the mass. If the patient is not rotated, then the motion response of the perilesional tissue can be expected to be different for palpations along different aspects of the mass.

Finally, the motion response of tissue to palpation may also be influenced by the character of the tissue adjacent to the mass, whether the mass is situated in a bed of soft fatty tissue or in an area of dense glandular tissue and the fatty constituency of the breast. For example, for the case of a hard inclusion embedded in an area of fatty tissue, the inclusion can be expected to deform less than the surrounding tissues as the tissue is compressed. Similarly, for the case of a soft tissue inclusion embedded in dense glandular tissue, the opposite will be true and the inclusion will absorb most of the deformation. The motion response to palpation will therefore also depend on the character of the surrounding parenchymal tissues (whether they are soft or stiff) and the relative difference between the tumor and tissue-elastic moduli. In our motion studies, we observed that larger displacements seemed to occur in patients with predominantly fatty breast parenchyma (patients 5 and 6), with smaller overall displacements observed in breast parenchyma containing predominantly glandular tissue or a mixture of fatty and glandular tissues (patients 1 to 4).

There is clearly a natural variability of motion responses from patient to patient. A more exhaustive study would have to take these differences into account to determine if these are indeed important variables. The results presented here represent a first step toward representing motion information in a more objective manner. The next step might be to attempt a normalization for major biophysical factors such as separation between driving surfaces on the skin, distance moved,

size and distance of masses from surface and basic tissue type surrounding masses. Whether standardization of the applied motion will be more effective than application of a maximum comfortable local stress and compensation with normalization remains to be seen.

Recent research has focused on the development of quantitative methods for applying more precise or known palpations for tumor elasticity measurement. Cespedes *et al.* (1993), in particular, have experimented with applying a known fixed and uniform compression to the breast using modified mammography equipment and others have designed a technique for interactively determining a good, high stress to be applied quantitatively (Fowlkes *et al.* 1995; Sarvazyan *et al.* 1995; Skovoroda *et al.* 1995). In addition, new techniques developed for three-dimensional motion tracking and strain imaging will help reduce problems in tracking and analyzing complex deformations and out-of-plane motions (Bertrand *et al.* 1989; Hein and O'Brien 1993; O'Donnell *et al.* 1994).

A new area of research in ultrasound is elasticity imaging. The basic idea in elasticity imaging is similar to displacement imaging. However, instead of tracking the motion of small regions of tissue the concept is to track dimensional changes in small areas or volumes of tissue as the tissue is compressed. The premise is that this can provide information about tissue mechanical properties. To measure area or volume changes in small rectangular regions of tissue speckle tracking, Fourier techniques have been applied to measure tissue displacement fields (O'Donnell *et al.* 1994; Ophir *et al.* 1991). Tissue displacement imaging thus also represents a necessary step in the elasticity imaging process.

The limited resolution of ultrasound does not allow imaging of any possibly invasive tentacles extending from a tumor site. However, imaging of tissue motion can provide important clues in the early detection of invasive tumor growth into surrounding tissues. Tissue displacement images of an invasive ductal carcinoma showed fixed translational motion of the surrounding parenchyma when the tumor was palpated, consistent with histological data and known physiological patterns of growth. Tissue displacement maps of benign fibrocystic masses exhibited slip motion that was present in all cases of fibrocystic disease.

Our present work is essentially based on the following facts and assumptions:

1. The presence of a stellate or star-shaped mass is one of the most distinct mammographic features of a breast malignancy.
2. Stellate neoplasms can alter tumor and connective tissue responses due to palpation compared to non-invaded tissues.

3. Ultrasound provides a means for quantitative imaging of internal tissue displacements.
4. Altered tumor and connective tissue responses can be quantified and potentially used for early detection and classification of breast cancers.

Acknowledgments—The authors would like to thank Debra Ikeda, M.D., for valuable assistance in recruiting patients and in acquiring ultrasound data and Rich Czerwinski and Scott Ellis for their help in digitizing ultrasound images and in the printing of the color images. This work was supported in part by National Institutes of Health Grant No. 5 T32 CA 09067 and by National Cancer Institute PHS Grant No. 5 RO1 CA55076.

REFERENCES

- Adler, R.; Rubin, J.; Bland, P.; Carson, P. Quantitative tissue motion analysis of digitized m-mode images: gestational differences of fetal lung. *Ultrasound Med. Biol.* 16:561–569; 1990.
- American Cancer Society. Cancer facts and figures. Technical report; 1991.
- Bamber, J.; Gonzalez, L.; Cosgrove, D.; Simmons, P.; Davey, J.; Mckinna, J. Quantitative evaluation of real-time ultrasound features of the breast. *Ultrasound Med. Biol.* 14:81–87; 1988.
- Berg, J. Clinical implications of risk factors for breast cancer. *Cancer* 53:589–591; 1984.
- Bertrand, M.; Meunier, J.; Doucet, M.; Ferland, G. Ultrasonic biomechanical strain gauge based on speckle tracking. In: Proceedings of the IEEE ultrasonics symposium. *IEEE Ultrason. Ferroelect. Freq. Control* 2:859–863; 1989.
- Bogaert, I.; Herman, J. Importance of spicules in clinical staging of carcinoma of the breast. *Surg. Gynecol. Obstet.* 144:356–358; 1977.
- Cespedes, I.; Ophir, J.; Ponnekanti, H.; Maklad, N. Elastography: elasticity imaging using ultrasound with application to muscle and breast in vivo. *Ultrason. Imag.* 15:73–88; 1993.
- Chen, E.; Hein, I.; Adler, R.; Carson, P.; O'Brien, W. A comparison of the motion tracking of ultrasonic b-mode tissue images with a calibrated phantom. In: Proceedings of the IEEE ultrasonics symposium. *IEEE Ultrason. Ferroelect. Freq. Control* (Orlando, FL), 1211–1214; 1991.
- Chen, E.; Jenkins, W.; O'Brien, W., Jr. Accuracy and precision of estimating tissue displacements from ultrasonic images. In Proceedings of the IEEE ultrasonics symposium. *IEEE Ultrason. Ferroelect. Freq. Control* (Tucson, AZ). 2:1069–1072; 1992.
- Chen, E.; Jenkins, W.; O'Brien, W., Jr. The impact of various imaging parameters on ultrasonic displacement and velocity estimates. *IEEE Trans. Ultrason. Ferroelect. Freq. Control* 41:293–301; 1994.
- Ciatto, S.; Morrone, D.; Catarzi, S.; Turco, M. R. D.; Bianchi, S.; Ambrogetti, D.; Cariddi, A. Radial scars of the breast: review of 38 consecutive mammographic diagnoses. *Radiology* 187:757–760; 1993.
- Fowlkes, J.; Emelianov, S.; Sarvazyan, A.; Skovoroda, A.; Pipe, J.; Adler, R.; Carson, P. Cancer detection using tissue elasticity imaging. *Med. Phys.* (in press); 1995.
- Gallagher, H. S.; Martin, J. M. Early phases in the development of breast cancer. *Cancer* 24:1170–1178; 1969.
- Gold, R. H.; Bassett, L. B. Mammography thermography and ultrasound in breast cancer detection. Grune & Stratton: New York; 1981.
- Hein, I.; O'Brien, W. Current time-domain methods for assessing tissue motion by analysis from reflected ultrasound echoes—a review. *IEEE Trans. Ultrason. Ferroelect. Freq. Control* 40:84–102; 1993.
- Heitzman, E. The lung: radiologic–pathologic correlations. St. Louis: Mosby, 1973.
- Kasumi, F.; Fukami, A.; Kuno, K.; Kajitani, T. Characteristic echographic features of circumscribed cancer. *Ultrasound Med. Biol.* 8:369–375; 1982.
- Kimme-Smith, C. National cancer institute breast imaging workshop. *AJR* 158:268; 1992.
- Krecke, K. N.; Gisvold, J. J. Invasive lobular carcinoma of the breast: mammographic findings and extent of disease at diagnosis in 184 patients. *AJR* 161:957–960; 1993.
- Leborgne, R. Diagnosis of tumors in of the breast by simple roentgenography: calcifications in carcinoma. *AJR* 65:1–11; 1951.
- Leibman, A. J.; Lewis, M.; Kruse, B. Tubular carcinoma of the breast: mammographic appearance. *AJR* 160:263–265; 1993.
- Leucht, W.; Rabe, D.; Humbert, K. Diagnostic value of different interpretative criteria in real-time sonography of the breast. *Ultrasound Med. Biol.* 14(suppl. 1):59–73.
- Martin, J.; Moskowitz, M.; Milbrath, J. Breast cancer missed by mammography. *AJR* 132:737–739; 1979.
- McLelland, R. Stellate lesions of the breast. *Recent Results Cancer Res.* 119:24–28; 1990.
- Monostori, Z.; Herman, P. G.; Carmody, D. P.; Eacobacci, T. M.; Capece, N. R.; Cruz, V. M.; Gentin, S.; Vernace, F. M. Limitations in distinguishing malignant from benign lesions of the breast by systematic review of mammograms. *Surg. Gynecol. Obstet.* 173:438–442; 1991.
- Moskowitz, M. Screening is not diagnosis. *Radiology* 133:265–268; 1979.
- O'Donnell, M.; Skovoroda, A.; Shapo, B.; Emelianov, S. Internal displacement and strain imaging using ultrasound speckle tracking. *IEEE Trans. Ultrason. Ferroelect. Freq. Control* 41:314–325; 1994.
- Ophir, J.; Cespedes, I.; Ponnekanti, H.; Yazdi, Y.; Li, X. Elastography: a quantitative method for imaging the elasticity of biological tissues. *Ultrason. Imag.* 13:111–134; 1991.
- Ramamurthy, B.; Trahey, G. Potential and limitations of angle-independent flow detection algorithms using radio frequency and detected echo signals. *Ultrason. Imag.* 13:252–268; 1991.
- Sarvazyan, A.; Skovoroda, A.; Emelianov, S.; Fowlkes, J.; Pipe, J.; Adler, R.; Buxton, R.; Carson, P. Biophysical bases of elasticity imaging. *Acoust. Imag.* (in press); 1995.
- Sickles, E. Mammographic features of early breast cancer. *AJR* 143:461–464; 1984.
- Skovoroda, A.; Emelianov, S.; Lubinski, M.; O'Donnell, M. Tissue elasticity reconstruction based on ultrasonic displacement and strain images. *IEEE Trans. Ultrason. Ferroelect. Freq. Control* (in press); 1995.
- Skovoroda, A.; Emelianov, S.; Lubinski, M.; Sarvazyan, A.; O'Donnell, M. Theoretical analysis and verification of ultrasound displacement and strain imaging. *IEEE Trans. Ultrason. Ferroelect. Freq. Control* 41:302–313; 1994.
- Tabar, I.; Dean, P. Teaching atlas of mammography. New York: Thieme-Stratton; 1985.
- Ueno, E. Classification and diagnostic criteria in breast echography. *Jpn. J. Med. Ultrason.* 13:19–31; 1986.
- Ueno, E. Lesion assessment by colour doppler. In: Jellins, J.; Rickard, M. T.; Madjar, H., eds. *IBUS breast ultrasound teaching session, International Breast Ultrasound School, Baden; 1993:34–37.*
- Ueno, E.; Tohno, E.; Soeda, S.; Asaoka, Y.; Itoh, K.; Bamber, J.; Blaszczyk, M.; Davey, J.; McKinna, J. Dynamic testing in real-time breast echography. *Ultrasound Med. Biol.* 14:53–57; 1988.
- Vlaisavljevic, V. Differentiation of solid breast tumors on the basis of their primary echographic characteristics as revealed by real time scanning of the uncompressed breast. *Ultrasound Med. Biol.* 14:75–80; 1988.
- Wolfe, J. (2nd ed.). *Xeroradiography of the breast* Springfield, IL: Charles C. Thomas.